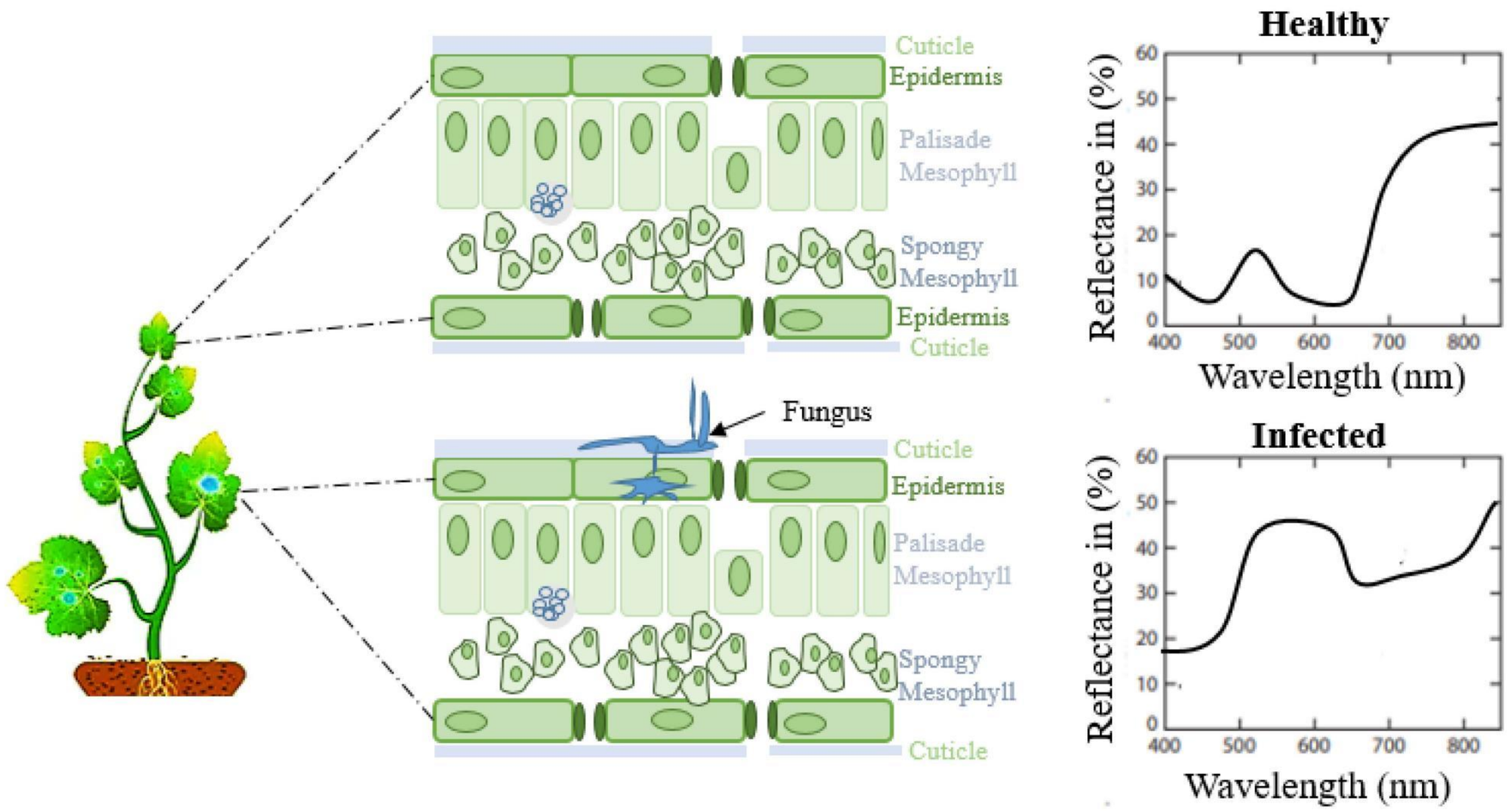

Fig. 4. Spectral reflectance characteristics with respect to the healthy or diseased status of a plant tissue [9], [144].

the pathogen–host interaction and the effect on plant tissues due to fungal diseases, genetic resistance of disease needs to be analyzed at the laboratories under hyperspectral microscopes [17]. However, the analyses of the individual organs such as root, stem, leaf, ear, and fruit need to be carried out in greenhouses, fields, and sometimes in laboratories to perform early disease detection. Canopy-level measurements are performed for severity assessment to translate the detected diseases into the severity ranks [17]. Canopy-level measurements indicate assessments at the plant canopy level, which includes all the leaves and stems above the ground [17]. The analysis of hyperspectral images of the entire canopy can aid the researchers in translating the detected disease symptoms into severity ranks and provides valuable insights into plant diseases [17]. The following case studies of selected plant diseases briefly discuss the application of hyperspectral images used for disease diagnosis.

1) Disease Detection: Early detection of plant diseases is essential in agronomy as necessary precautions can be taken to prevent the spread. The hyperspectral image analysis aims to detect the infected plants for the type of diseases, early symptoms, and kinetics. Fig. 4 shows the spectral characteristics of healthy and infected plants.

Canada is the second largest wheat exporter in the world. A recent report from 2020 shows that Canada has produced over 35 million metric tons of wheat in the year 2020 [294]. Fusarium head blight is a common fungal disease that reduces wheat yield as it directly affects the ears and the stalks of the wheat plant. A study in [295] compared different imaging technologies such as chlorophyll fluorescence imaging, infrared thermography, and hyperspectral imaging using time-series measurement. The acquired hyperspectral images could aid in identifying the Fusarium blight head infection and noninoculated spikes of the wheat head from the third day [295] with 78% of disease detection accuracy. Yellow rust is also one of the diseases that can cause a drastic impact on the yield. Ashourloo et al. [148] proposed multivariate methods, which involve partial linear regression, support vector regression, and gaussian process regression to identify the yellow rust diseases at the leaf and canopy level. The results showed promising performance in detecting diseases at an early stage. Bohnenkamp et al. [144] conducted an experiment to detect yellow rust and brown rust on wheat plants from hyperspectral images of wheat leaves. The investigation was conducted in a laboratory at the leaf level and with controlled environmental conditions. The images are analyzed by using least-squares factorization so that the spectral information for yellow and brown rust can be identified. This study aided in understanding the pathogenic properties of the diseases by using an explicable disintegration of the spectral reflectance analysis [144]. Powdery mildew is another contagious disease in wheat plants that starts as light white pustules on wheat leaves. However, very few studies were conducted to detect powdery mildew diseases from the hyperspectral images. One such study was conducted at the Beijing Academy of Agriculture and Forestry Sciences Field. The study collected 114 plant leaf samples, including infected leaves (80 leaves) and healthy leaves (34 leaves), by remote sensing devices. The images were then analyzed using regression models, which could detect the leaf diseases very well [296]. One study regarding the leaf spot disease for maize was conducted in [151]. The experiment was carried out with an Analytical Spectral Device FieldSpec 3spectrometer in a Cedara experimental field area of South Africa. Two spectral regions, 350–1000 nm and 1000–2500 nm spectral regions, were chosen for leaf sampling. A guided regularized RF

Authorized licensed use limited to: FUDAN UNIVERSITY. Downloaded on August 28,2025 at 01:49:24 UTC from IEEE Xplore. Restrictions apply.